Accepted Manuscript

Global Optimisation of Multi-Plant Manganese Alloy Production

Martin Naterstad Digernes, Lars Rudi, Henrik Andersson,
Magnus Stålhane, Stein O. Wasbø, Brage Rugstad Knudsen

PII: S0098-1354(17)30425-8
DOI: 10.1016/j.compchemeng.2017.12.001
Reference: CACE 5968

To appear in: *Computers and Chemical Engineering*

Received date: 2 August 2017
Revised date: 1 December 2017
Accepted date: 3 December 2017

Please cite this article as: Martin Naterstad Digernes, Lars Rudi, Henrik Andersson, Magnus Stålhane, Stein O. Wasbø, Brage Rugstad Knudsen, Global Optimisation of Multi-Plant Manganese Alloy Production, *Computers and Chemical Engineering* (2017), doi: 10.1016/j.compchemeng.2017.12.001

This is a PDF file of an unedited manuscript that has been accepted for publication. As a service to our customers we are providing this early version of the manuscript. The manuscript will undergo copyediting, typesetting, and review of the resulting proof before it is published in its final form. Please note that during the production process errors may be discovered which could affect the content, and all legal disclaimers that apply to the journal pertain.

ACCEPTED MANUSCRIPT

Highlights

- A nonlinear pooling-type optimization model for manganese alloy production.
- Application of Multiparametric Disaggregation Technique on large-scale nonlinear pooling problem.
- Presentation of industrial case study from the manganese alloy producer Eramet Norway.

ACCEPTED MANUSCRIPT

ACCEPTED MANUSCRIPT

Global Optimisation of Multi-Plant Manganese Alloy Production

Martin Naterstad Digernes[a,1], Lars Rudi[a,1],
Henrik Andersson[a], Magnus Stålhane[a], Stein O. Wasbø[b], Brage Rugstad Knudsen[b,c,d,*]

[a]*Department of Industrial Economics and Technology Management, NTNU, Alfred Getz veg 3, NO-7491 Trondheim, Norway*
[b]*Cybernetica AS, Leirfossveien 27, NO-7038 Trondheim, Norway*
[c]*Department of Engineering Cybernetics, NTNU, O. S. Bragstads plass 2D, NO-7491 Trondheim, Norway*
[d]*SINTEF Energy Research, Sem Sælandsvei 11, NO-7465 Trondheim, Norway*

Abstract

This paper studies the problem of multi-plant manganese alloy production. The problem consists of finding the optimal furnace feed of ores, fluxes, coke, and slag that yields output products which meet customer specifications, and to optimally decide the volume, composition, and allocation of the slag. To solve the problem, a nonlinear pooling problem formulation is presented upon which the bilinear terms are reformulated using the Multiparametric Disaggregation Technique (MDT). This enables global optimisation by means of commercial software for mixed integer linear programs. We demonstrate the model and solution approach through case studies from a Norwegian manganese alloy producer. The computational study shows that the model and proposed optimisation approach can solve problem sizes of up to ten furnaces to a small optimality gap, that global optimization approach with MDT scales well with larger, real problem instances, and that the model outperforms the current operational practice.

Keywords: Manganese Alloy Production, Pooling Problem, Multiparametric Disaggregation Technique, Global Optimisation, Multi-plant Production, Mixed Integer Linear Programming

1. Introduction

Manganese is a hard, brittle, silvery metal that occurs in nature in the form of minerals, mainly as oxides. It is an essential element in steel and aluminium alloys, commonly used in railway tracks and safes, and beverage cans and kitchenware, respectively. The total production of manganese alloys has been approximately twenty million tonnes annually in the recent years *(d'Haramb ure, 2015)*. An average price of manganese alloys around 2 USD/kg *(InvestmentMine, 2017)* makes the manganese alloy production a multi-billion dollar industry.

Manganese alloy production can be divided into two categories: extraction and smelting. Extraction constitutes the processes of mining, hauling the ore to a processing plant, crushing, separation and beneficiation at the plant, transportation to sinter plants, and sintering *(Olsen et al., 2007)*. The smelting process constitutes the processes of

*Corresponding author
Email address: brage.knudsen@sintef.no (Brage Rugstad Knudsen)
[1]The first two authors contributed equally to this paper.

ACCEPTED MANUSCRIPT

smelting ores, fluxes, quartz, and coke in furnaces, tapping and casting, refining, crushing, and transportation of by-products back into processes or to disposal sites *(International Manganese Institute and Hatch, 2015)*.

The focus of this paper is on the smelting process of the manganese alloy supply-chain. Current operational practice in this sector is largely based on process operators' experience and process knowledge, where emphasis is put on stable and efficient production of each individual plant and furnaces, with little integration of the overall multi-plant structure. The literature on manganese production optimisation is limited. To the authors' knowledge, only one article exists on the topic. *Jipnang et al. (2013)* present a single high-carbon ferromanganese (HC FeMn) and medium-carbon silicomanganese (MC SiMn) furnace process-optimisation model, based on mass and energy balances. The model only focuses on the production specific aspects of the problem, and optimises a target function such as total operating costs, energy consumption, Mn recovery, or the amount of slag produced from the furnace. The model relies on proprietary software, thereby hiding the modell applied. It is capable of calculating the production for single HC FeMn and MC SiMn furnaces, respectively, and the paper states that connecting the two processes and adding possibilities for different production strategies are considered future research *(Jipnang et al., 2013)*. An optimisation model that considers the integrated production of FeMn and SiMn alloys across multiple plants can hence advance both current practice and targeted optimisation of the production planning. To this end, a multi-plant manganese alloy production-planning problem consists of optimizing the mixing of raw materials and composition of end-products satisfying the demand and given quality specifications, while incorporating the possibility of transporting by-products and other materials between the furnaces and plants to reduce costs and improve profit for the company. In the remainder of the paper, this considered problem is denoted as the Manganese Alloy Multi-plant Production (MAMP) problem.

Production of manganese alloys resorts to smelting of raw materials in furnaces, with flows of output by-products between the furnaces. This structure enables the MAMP problem to be formulated as a nonlinear pooling problem, with intermediate pools present in the form of furnaces and refining stations. The raw material inventories are sources and end- and by-product inventories are terminals. The pooling problem is a generalisation of the blending problem introduced by *Haverly (1978)*, and is used to model systems that have intermediate mixing pools in the blending process of streams with varying qualities and volumes *(Audet et al., 2004)*. A complicating element for the MAMP problem, however, is that intermediate pools are coupled as a result of utilisation of by-products.

The pooling problem arises in a variety of industries including oil refining *(Ben-Tal et al., 1994; Amos et al., 1997)*, mining industry *(Boland et al., 2015)*, and wastewater network problems *(Meyer and Floudas, 2006; Jezowski, 2010)*. Blending stream qualities results in nonlinear terms in the pooling problem formulation, yielding a nonconvex nonlinear program (NLP) *(Audet et al., 2004; Alfaki, 2012)*. These pooling problems, also classified as bilinear process networks, are generally difficult to solve to global optimality since bilinear constraints are required to model the mixing of different streams *(Kolodziej et al., 2013b)*. Multiple optimisation formulations of the pooling problem are found in the literature. Formulating the standard pooling problem in different ways have varying ramifications for the problem size and relaxation tightness, although the formulations are mathematically equivalent *(Misener and Floudas, 2009)*.

ACCEPTED MANUSCRIPT

The most common formulations for the standard and generalised pooling problem are the P-formulation *(Haverly, 1978)*, the Q-formulation *(Ben-Tal et al., 1994)*, and the PQ-formulation *(Quesada and Grossmann, 1995; Sherali et al., 1998; Tawarmalani and Sahinidis, 2002)*.

Solution methods for the pooling problem can generally be classified into local and global optimisation methods *(Alfaki and Haugland, 2013)*. Guaranteeing global optimality is of major importance, as the objective function typically is related to an economic metric *(Teles et al., 2012)*. A summary of some of the different solution methods can be found in *Misener and Floudas (2009)*, including Successive Linear Programming (SLP), Lagrangian approaches, the Reformulation Linearisation Technique (RLT), and different branch-and-bound schemes.

A relatively recent solution method to pooling problems is the Multiparametric Disaggregation Technique (MDT) *(Teles et al., 2012, 2013; Kolodziej et al., 2013a,b)*. The method relies on a concept based on the characteristics of the decimal representation of real numbers. The NLP is transformed into a suitably reformulated problem containing new sets of continuous and discrete variables. By disaggregating and parameterising the variables in the nonlinear terms, it is shown how to approximate the original NLP formulation as a mixed integer linear program (MILP). The quality of the solution depends on the number of significant digits used to represent the number *(Teles et al., 2012)*.

Nonconvex NLPs with multiple local optima may renders the use of conventional NLP solvers ineffective *(Teles et al., 2012; Wicaksono and Karimi, 2008)*. On the other hand, general-purpose global optimization solvers may scale poorly with larger problem sizes, as they lack the capability of exploiting special structures of the nonconvexities in classes of problems such as the pooling problem. *Kolodziej et al. (2013a)* show that the MDT relaxation applied to large problems compares favorably with general global optimisation solvers. They also show that the solution from the upper and lower bounding formulations converge towards the original nonlinear formulation in the limit of an infinite number of discretisation intervals. Compared to spatial branch-and-bound involving a continuous relaxation, the MDT involves a discrete partition of the feasible region. This partitioning means one can use standard MILP solvers to generate an ϵ-optimal solution, given that one exists for the selected accuracy settings. Further, the MDT does not require the specification of an initial point *(Teles et al., 2012)*, and has been demonstrated to scale well with increasing problems sizes (Castro and Teles, 2013). For these reasons, the MDT is selected to be the method for reformulating the bilinear constraints present in the MAMP.

The main contribution of this paper is the formulation of an optimisation model for decision support of multi-plant manganese alloy production planning. The optimisation model is tested on a case study based on the plant locations and furnace setup of Eramet Norway. Further contributions include (I) a general, nonlinear formulation of the problem in consideration, applicable to any alloy production with similar processes as manganese alloy production, and (II) a demonstration of the MDT to solve a large-scale industrial pooling problem. The remainder of the paper is organised as follows. First, a brief introduction to the manganese alloy production problem is given. Then, the mathematical model is presented and the bilinear constraints in the pooling problem are reformulated using the MDT. Finally, a computational study is conducted based on a realistic case, followed by results, concluding remarks, and considerations for future research.

ACCEPTED MANUSCRIPT

2. Problem Description

A manganese alloy manufacturer has a set of furnaces located at plants to produce manganese alloys. The alloys produced are given by customer specifications. The production is, therefore, based on contracts that must be satisfied. Customer specifications include order volume and alloy composition, resulting in a wide range of possible order sizes and end-products. To meet the end-product specifications, a set of raw materials, including ores, fluxes, and coke sources, containing different concentrations of various elements and oxides is available to the production. The raw materials are blended in the furnaces and further processed to produce the desired end-products. Any excess end-product produced can be sold on optional contracts in the spot market or held as an inventory. Producing manganese alloys also yields various by-products, where some are valuable and may be sold.

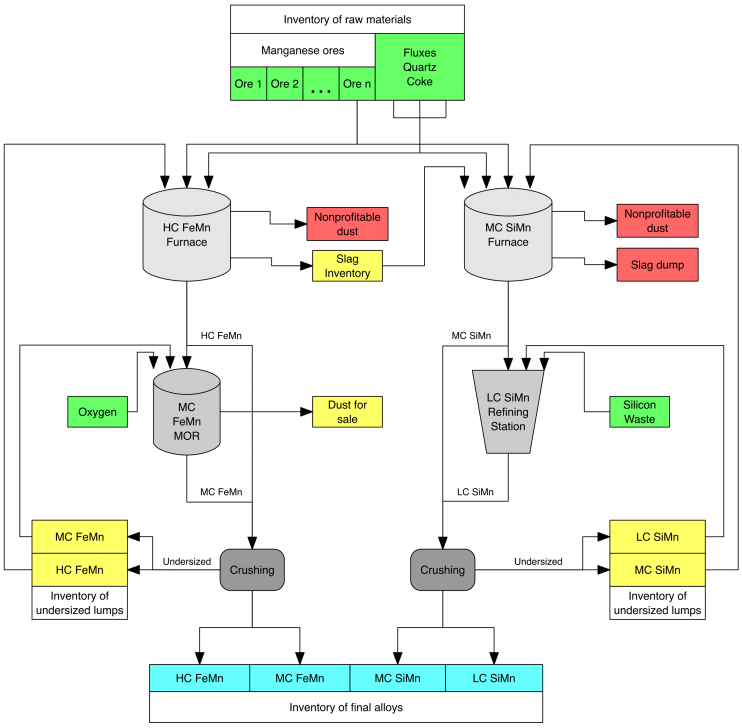

Figure 1: Overview of the material flow in manganese alloy production using the duplex method. Green colour: raw materials. Red: wastes. Yellow: inventory of reusable/saleable materials. Blue: end-products. Scales of grey: the furnace, refining, and crushing processes.

Figure 1 provides an overview of the processes and material flow in a manganese alloy plant producing several grades of both ferro and silico manganese. The raw material inventory supplies the necessary resources to the HC FeMn and MC SiMn furnaces. The output from the furnaces are Mn alloys, slag, and dust. The Mn alloys are either crushed into end-products or refined into low carbon (LC) or medium carbon (MC) products. Refining by Manganese Oxygen Refining (MOR) also produces metal-oxide dust as a salable by-product. The liquid alloys are solidified before crushing

ACCEPTED MANUSCRIPT

to end-products of different sizes. End-products are stored at sales inventories, while undersized lumps fines are kept at inventories and reused or sold at reduced price. The slag produced by HC FeMn furnaces can either be discarded or reused to save raw material costs in the MC SiMn furnaces, the latter being the common industry practice. This practice is called the duplex method *(Olsen et al., 2007)* and couples the otherwise independent production paths. Both slag-to-metal ratio and slag composition can be manipulated through ore combinations and furnace temperatures, thereby potentially achieving a more efficient production by blending slags from different HC FeMn furnaces in the MC SiMn furnaces. As both furnace types are not necessarily located at the same plant, slag must be transported between plants. Thus, the decision-making process is complicated by the slag-to-metal-ratio, the slag composition, and the volume of slag to send to each MC SiMn furnace from each HC FeMn furnace. The furnaces used to smelt the raw materials can produce both HC FeMn and MC SiMn alloys, but only one alloy type at a time. Each furnace has a mass and electrical power capacity that limits the raw material feed to the furnace. The furnaces also have limitations on the amount of fines it is possible to feed, since feeding too much fines (or undersized lumps) may lower the furnace temperature and thereby impede efficient furnace operations.

The MAMP problem must include mass and energy balances for each furnace. Smelting of ores with addition of fluxes and coke to produce silico and ferroalloys constitutes highly complex chemical processes occurring over a wide range of temperatures. Imposing the full mass and energy balance for all elements present in the ores, slags and end-products is therefore intractable for multi-plant production planning. Still, only a subset of all present elements in the furnace processes, in particular Mn, Fe, Si, C, Al, Mg, Ca, and their associated oxides, is essential for deciding the optimal blend and thereby compute good solutions to the production-planning problem. To this end, we include the mass and energy balances for the reactions of these main elements, provided in reactions (70)–(82) in Appendix A. We assume that all reactions are steady state and hence that the chemical reactions in the appendix are complete.

The set of reactions taking place in the furnaces are both exothermic and endothermic, while the overall process is strongly endothermic. HC FeMn production has a typical overall electrical energy consumption of 2500kWh per tonnes of alloy produced. For MC SiMn, the same number is about 4500kWh/tonnes. The electrical power consumption of the furnaces is therefore an important cost driver in manganese alloy production, by the raw material composition affecting the electrical energy consumption, and with almost twice as high electricity cost for producing MC SiMn compared with HC FeMn. The energy consumption in a furnace is determined by the net effect of exothermic and endothermic reactions and the enthalpy of the materials entering and leaving the furnace *(Olsen et al., 2007)*. The total enthalpy consists of formation enthalpy and sensible enthalpy. An approximate electric power consumption is then given by

$$\bar{P} = (H^{\mathrm{F}}_{\mathrm{out}} + H^{\mathrm{S}}_{\mathrm{out}}) - (H^{\mathrm{F}}_{\mathrm{in}} + H^{\mathrm{S}}_{\mathrm{in}}) + Q^{\mathrm{loss}} \tag{1}$$

where $H^{\mathrm{F}}_{\mathrm{out}}$ represents the formation enthalpy and $H^{\mathrm{S}}_{\mathrm{out}}$ the sensible enthalpy of the resultants at the exit temperature, $H^{\mathrm{F}}_{\mathrm{in}}$ the formation enthalpy and $H^{\mathrm{S}}_{\mathrm{in}}$ the sensible enthalpy of the reactants at the entry temperature, Q^{loss} the net heat-loss to the surroundings, and $\bar{P}$ the electricity (work) fed to the furnaces. Gas emissions, both from CO, CO_2, and vaporised H_2O constitute a significant part of the furnace power consumption *(Olsen et al., 2007)*.

ACCEPTED MANUSCRIPT

Refining stations are required to produce MC FeMn and LC SiMn products. These refining units have a mass and energy capacity limiting the feed to each process. Each plant has inventories for storing resources and end-products, which at each plant are divided into raw material inventories, recycling materials inventories, and end-product inventories. All inventories have capacity limits. The slag produced by the furnaces is a proportion to the metal produced, and this ratio can fluctuate between a lower and upper bound dependent on the raw materials used for a specific alloy and slag. Slag compositions may vary in each HC FeMn furnace. The reuse of HC FeMn slag in MC SiMn furnaces is the main coupling between the FeMn and SiMn productions. Slag from the MC SiMn furnaces and the nonprofitable dust produced by both furnace types is discarded.

Revenues and costs are linked to various parts of the production. The resources used in the production, except the undersized lumps, are associated with a procurement cost. Smelting the raw materials in the furnaces requires energy in the form of electricity. Thus, the furnace process incurs electricity costs. Reusing slag produced by HC FeMn furnaces in MC SiMn furnaces at other plants incurs a transportation cost per tonne slag transported. Slag from the HC FeMn furnaces can also be discarded instead of reused, which incurs a discard cost. The other by-products that must be discarded also incur a discard cost. The metallic-oxide dust from the MOR process is associated with a revenue since it can be sold. Each end-product is associated with a revenue per tonne sold on fixed contracts or in the spot market.

The objective of the MAMP problem is to optimise the integrated production of FeMn and SiMn alloys across multiple plants to maximise profit. The profit is determined by deciding the optimal volumes of end-products to produce by mixing raw materials, while satisfying given quality specifications. Production costs are considerable, and the MAMP problem should, therefore, ensure optimal use of raw materials to the furnaces and refining processes. The solution to the MAMP problem should also describe the optimal slag volume and slag composition to be produced in the HC FeMn furnaces and the allocation of slag to the MC SiMn furnaces.

3. Mathematical Formulation

Multi-plant production, blending, advanced chemistry, and the coupling of the FeMn and SiMn productions that make up the MAMP problem add a high degree of complexity to the formulation of the problem. To reduce the scope of the problem, model assumptions are made. The MAMP problem is solved once and the production plan given by the solution can be used for the given planning period. The end-product demands are assumed to originate from fixed contracts and a spot market. Fixed contracts are known a priori and the demanded chemical compositions are given. The excess production can be sold on the spot market up to a limit. The raw material procurement prices, electricity prices, and end- and by-product sales prices are constant. Switching furnace settings or switching furnaces on and off are not included in the model.

There is an initial inventory of raw materials at each plant. The reuse of undersized lumps must be balanced so the process cannot consume more undersized lumps than it produces. The feed of undersized lumps is therefore bounded by the produced volume of undersized lumps. We assume fixed amounts of crushed product that ends up as undersized

ACCEPTED MANUSCRIPT

lumps and the percentage of the total feed to the processes that ends up as by-products.

A large set of chemical reactions is involved in the production of manganese alloys. The model includes the main reactions occurring in the furnaces to ensure the correct weight fractions of elements in the final alloy. All chemical reactions are assumed to be complete. The reactions (70) - (82) in Appendix A therefore translate into linear equality constraints. In practice, many complicated and incomplete chemical reactions happen in the furnace. However, for simplicity, the slag is set to only consist of the most important oxides in the model. These oxides are MnO, FeO, SiO_2, Al_2O_3, MgO, and CaO.

Process metallurgists typically want to determine a range of slag compositions, given by the lime basicity *(Olsen et al., 2007)*, to ensure a suitable viscosity of the slag. These considerations are imposed through constraints on the slag composition. The specific carbon content of a end-product is only considered within medium and high range for FeMn and low and medium range for SiMn. Detailed classifications of product types by percentage carbon content within these ranges are disregarded, yielding a reduced set of end-products.

The model is flow- and quality-based specifically developed for manganese alloy multi-plant production.We use the P-formulation (Haverly, 1978), as this is the most common formulation used in the chemical processing industry and it provides an intuitive understanding of the process flows and their qualities for this new problem.

Table 1: Sets and indices

Set	
$\mathcal{P}$	Set of plants, indexed by p, g
$\mathcal{F}_p$	Set of furnaces at plant p, indexed by f, t
$\mathcal{E}$	Set of end-products, indexed by e
$\mathcal{B}$	Set of by-products, indexed by b
$\mathcal{R}$	Set of raw materials, indexed by r, ρ
$\mathcal{K}$	Set of elements and oxides, indexed by k
$\mathcal{C}$	Set of chemical reactions, indexed by c
$\mathcal{V}$	Set of variables in the chemical reactions, indexed by v
$\mathcal{F}_p^{\text{FeMn}}$	Subset of all HC FeMn furnaces at plant p, $\mathcal{F}_p^{\text{FeMn}} \subseteq \mathcal{F}_p$
$\mathcal{F}_p^{\text{SiMn}}$	Subset of all MC SiMn furnaces at plant p, $\mathcal{F}_p^{\text{SiMn}} \subseteq \mathcal{F}_p$
$\mathcal{C}^{\text{O}}$	Subset of original chemical reactions, $\mathcal{C}^{\text{O}} \subset \mathcal{C}$
$\mathcal{C}^{\text{C}}$	Subset of critical chemical reactions, $\mathcal{C}^{\text{C}} \subset \mathcal{C}$
$\mathcal{C}^{\text{S}}$	Subset of slag chemical reactions, $\mathcal{C}^{\text{S}} \subset \mathcal{C}$
$\mathcal{K}^{\text{C}}$	Subset of critical elements and oxides,$\mathcal{K}^{\text{C}} \subset \mathcal{K}$
$\mathcal{K}^{\text{G}}$	Subset of gases, $\mathcal{K}^{\text{G}} \subset \mathcal{K}$
$\mathcal{K}^{\text{S}}$	Subset of elements and oxides in the slag, $\mathcal{K}^{\text{S}} \subset \mathcal{K}$

Table 2: Parameters

Parameter	
A_{fkcv}	Constant for an element or oxide k in chemical reaction c for variable v in furnace f.

ACCEPTED MANUSCRIPT

A^{LS}_{fkcv}	Constant for an element or oxide k in the left side ratio equation for chemical reaction c for variable v in furnace f.
A^{RS}_{fkcv}	Constant for an element or oxide k in the right side ratio equation for chemical reaction c for variable v in furnace f.
B_{fkc}	1 if an element or oxide k exist in chemical equation c for furnace f, 0 otherwise.
C_r	Procurement cost per tonne raw material r.
C^{E}	Electricity cost per kWh.
C^{LSiL}	Cost per tonne LC SiMn undersized lumps used.
C^{MFeL}	Cost per tonne MC FeMn undersized lumps used.
C^{O}	Cost per tonne oxygen used. This includes procurement and electricity cost.
C^{S}	Discard cost per tonne slag.
C^{SiW}	Cost per tonne silicon waste used. This includes procurement and electricity cost.
C^{T}_{pg}	Transportation cost per tonne slag from plant p to plant g.
D^{F}_{e}	Fixed contract demand for end-product e.
D^{O}_{e}	Spot market limit for end-product e.
H^{F}_{k}	Formation enthalpy for each element or oxide k, in kJ/tonne.
H^{S}_{k}	Sensible enthalpy for each element or oxide k, in kJ/tonne.
I_{pr}	Initial inventory of raw material r at plant p in tonnes.
I^{LSiL}_{p}	Initial inventory of LC SiMn undersized lumps at plant p in tonnes.
I^{MFeL}_{p}	Initial inventory of MC FeMn undersized lumps at plant p in tonnes.
I^{O}_{p}	Initial inventory of oxygen at plant p in tonnes.
I^{SiW}_{p}	Initial inventory of silicon waste at plant p in tonnes.
L^{H}	Furnace heat loss factor.
M_k	Molar mass in moles per tonne for element or oxide k.
Q^{F}_{pf}	Total capacity of furnace f at plant p in tonnes.
Q^{MOR}_{p}	Total MOR capacity at plant p in tonnes.
Q^{REF}_{p}	Total LC SiMn refining station capacity at plant p in tonnes.
R^{B}_{b}	Revenue or discard cost per tonne of by-product b.
R^{F}_{e}	Fixed contract revenue per tonne end-product e sold.
R^{O}_{e}	Spot price per tonne end-product e sold on the spot market.
T_{kcv}	1 if element or oxide k exist in chemical equation c for variable v, 0 otherwise.
$\underline{\Lambda}$	Lower limit on the weight percentage for slag production in an HC FeMn furnace.
$\overline{\Lambda}$	Upper limit on the weight percentage for slag production in an HC FeMn furnace.
Υ	Degree of pre-reduction in the HC FeMn furnaces.
$\underline{\Phi}_k$	Lower limit on the weight percentage for element or oxide k in slag.
$\overline{\Phi}_k$	Upper limit on the weight percentage for element or oxide k in slag.
Ψ^{B}_{fbk}	Weight percentage of element or oxide k in by-product b from furnace f.
$\Psi^{\mathrm{CRUSH}}_{b}$	Weight percentage of by-product b from the crushing process.
Ψ^{FeMn}_{k}	Weight percentage of element or oxide k in HC FeMn.
Ψ^{LSiL}	Weight percentage LC SiMn undersized lumps allowed to feed LC SiMn refining station.
Ψ^{MFeL}	Weight percentage MC FeMn undersized lumps allowed to feed MOR.
Ψ^{MOR}_{b}	Weight percentage of by-product b from MOR.
Ψ^{R}_{rk}	Weight percentage of element or oxide k in raw material r.
Ψ^{SiMn}_{k}	Weight percentage of element or oxide k in MC SiMn.
Ψ^{UL}	Weight percentage of undersized lumps allowed to feed a furnace.

ACCEPTED MANUSCRIPT

Ω^{MOR}	Oxygen-HC FeMn weight relationship factor.
Ω^{REF}	Silicon-MC SiMn weight relationship factor.

Table 3: Variables

Variable	
a_p	Tonnage of LC SiMn undersized lumps used in the LC SiMn refining station at plant p.
c_p	Tonnage of MC FeMn undersized lumps used in MOR at plant p.
e_{pf}	Electric power consumed by furnace f at plant p, in kWh.
g_e^{F}	Sale of end-product e made on fixed contracts.
g_e^{O}	Sale of end-product e on the spot market.
h_p	Tonnage of LC SiMn produced at plant p sent to crushing.
m_{pf}	Tonnage of alloy produced in furnace f at plant p sent to refining processes.
n_{pfkcv}	Moles of element or oxide k in furnace f at plant p in equation c for variable v.
o_p	Tonnage oxygen fed to the MOR at plant p.
q_{pf}	Tonnage slag produced in furnace f at plant p.
s_p	Tonnage silicon fed to the LC SiMn refining at plant p.
u_{pf}	Tonnage of alloy produced in furnace f at plant p sent to crushing.
x_{pe}^{E}	Tonnage of end-product e produced at plant p.
x_{pb}^{B}	Tonnage of by-product b produced at plant p.
y_{pfr}	Tonnage of raw material r fed to furnace f at plant p.
α_{pfkc}	Moles of element or oxide k in chemical equation c extracted as slag from furnace f at plant p.
σ_{pfgt}	Tonnage slag sent from furnace f at plant p to furnace t at plant g.
ϕ_{pfk}	Weight percentage of element or oxide k in the slag produced by furnace f at plant p.

Figure 2 illustrates the material flow within a plant and which processes the variables are describing, using a simplified superstructure. As an example, the variables y_{pfr} and n_{pfkcv} are related to the feeding of the furnaces from the raw material inventory, while a_p and s_p are related to the feeding of the LC SiMn refining station from refining resources. ϕ_{pfk}, e_{pf}, g_e^{F}, and g_e^{O} are not included in the figure since these are quality variables and not flow variables. The MAMP problem is, however, defined for multiple plants. Slag can be sent from an HC FeMn furnace at one plant to multiple MC SiMn furnaces, at the same plant or other plants.

ACCEPTED MANUSCRIPT

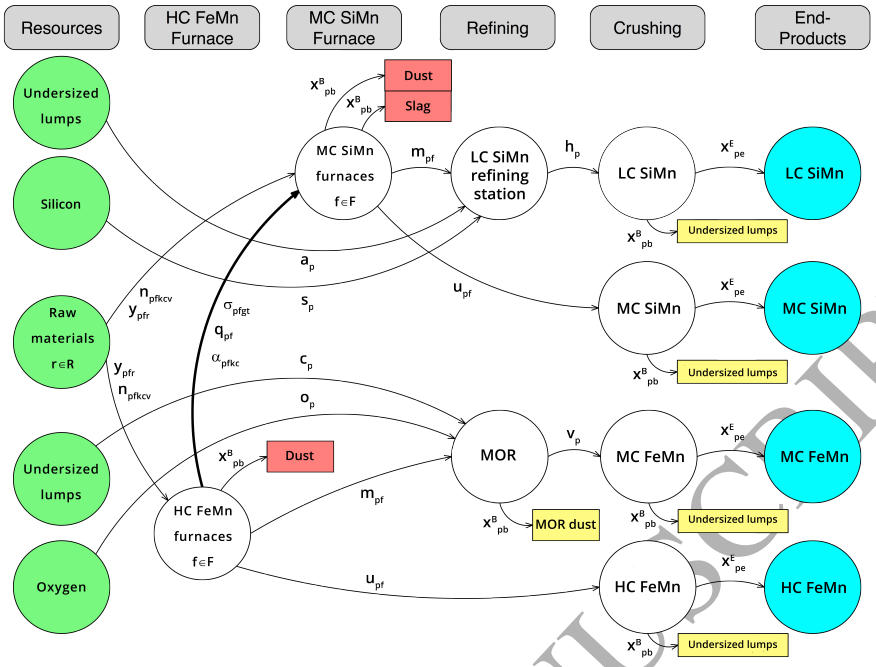

Figure 2: The MAMP superstructure for one plant. The same colour coding is applied as in Figure 1. Green: raw materials. Red: wastes. Yellow: inventory of reusable/saleable materials. Blue: final alloys.

3.1. Model

$$\max z = \sum_{e\in\mathcal{E}}(R_e^{\mathrm{F}} g_e^{\mathrm{F}} + R_e^{\mathrm{O}} g_e^{\mathrm{O}}) + \sum_{p\in\mathcal{P}}\sum_{b\in\mathcal{B}} R_b^{\mathrm{B}} x_{pb}^{\mathrm{B}} - \sum_{p\in\mathcal{P}}\sum_{f\in\mathcal{F}_p}\sum_{r\in\mathcal{R}} C_r y_{pfr} - \sum_{p\in\mathcal{P}}\sum_{f\in\mathcal{F}_p} C^{\mathrm{E}} e_{pf} - \sum_{p\in\mathcal{P}}(C^{\mathrm{O}} o_p + C^{\mathrm{MFeL}} c_p)$$
$$- \sum_{p\in\mathcal{P}}(C^{\mathrm{SiW}} s_p + C^{\mathrm{LSiL}} a_p) - \sum_{p\in\mathcal{P}}\sum_{f\in\mathcal{F}_p^{\mathrm{FeMn}}}\sum_{g\in\mathcal{P}}\sum_{t\in\mathcal{F}_g^{\mathrm{SiMn}}} C_{pg}^{\mathrm{T}}\sigma_{pfgt} - \sum_{p\in\mathcal{P}}\sum_{f\in\mathcal{F}_p^{\mathrm{FeMn}}} C^{\mathrm{S}}(q_{pf} - \sum_{g\in\mathcal{P}}\sum_{t\in\mathcal{F}_g^{\mathrm{SiMn}}}\sigma_{pfgt}) \quad (2)$$

The objective function 2 maximises the total profit from selling end- and by-products from manganese alloy production. It consists of revenue generated by selling end-products and selling and discarding by-products. It also include cost of raw materials, electricity cost, cost of oxygen and MC FeMn undersized lumps added to the MOR process and cost of silicon waste and LC SiMn undersized lumps added to the LC SiMn refining station process. Finally, total slag transportation cost between plants and cost of discarding the slag that is not re-used are subtracted.

To enhance readability and the understanding of which constraints restrict each process stage, the constraints are presented in different sections. The sections are presented in order of process stage according to Figure 2.

Resource inventory

$$\sum_{f\in\mathcal{F}_p} y_{pfr} \leq I_{pr} \qquad p\in\mathcal{P},\ r\in\mathcal{R} \quad (3)$$

ACCEPTED MANUSCRIPT

$$o_p \leq I_p^{\mathrm{O}} \qquad p \in \mathcal{P} \quad (4)$$

$$s_p \leq I_p^{\mathrm{SiW}} \qquad p \in \mathcal{P} \quad (5)$$

$$c_p \leq I_p^{\mathrm{MFeL}} \qquad p \in \mathcal{P} \quad (6)$$

$$a_p \leq I_p^{\mathrm{LSiL}} \qquad p \in \mathcal{P} \quad (7)$$

Constraints (3) - (7) are resource inventory constraints limiting the feed of particular resources to within the initial inventories of the respective resources.

Furnace constraints

$$\sum_{r\in\mathcal{R}} y_{pfr} + \sum_{k\in\mathcal{K}^{\mathrm{S}}}\sum_{c\in C^{\mathrm{S}}} M_k n_{pfkcv} \leq Q_{pf}^{\mathrm{F}} \qquad p \in \mathcal{P},\ f \in \mathcal{F}_p,\ v \in \{\mathrm{SLAG}\} \quad (8)$$

$$y_{pfr} \leq \Psi^{\mathrm{UL}} \sum_{\rho\in\mathcal{R}\setminus r} y_{pf\rho} \qquad p \in \mathcal{P},\ f \in \mathcal{F}_p,\ r \in \{\mathrm{HC\ FeMn}, \mathrm{MC\ SiMn}\} \quad (9)$$

$$\begin{aligned}
&\sum_{r\in\mathcal{R}}\sum_{k\in\mathcal{K}} \Psi_{rk}^{\mathrm{R}} y_{pfr} + \sum_{k\in\mathcal{K}^{\mathrm{S}}}\sum_{c\in C^{\mathrm{S}}} M_k n_{pfkc,\mathrm{SLAG}} + \sum_{c\in C^{\mathrm{O}}} M_{\mathrm{O}} n_{pf,\mathrm{CO_2},c,\mathrm{TOT}} \\
&+ \sum_{c\in C^{\mathrm{O}}} M_{\mathrm{CO}} n_{pf,\mathrm{CO},c,\mathrm{TOT}} - \sum_{b\in\mathcal{B}}\sum_{k\in\mathcal{K}}\sum_{r\in\mathcal{R}} \Psi_{fbk}^{\mathrm{B}} \Psi_{rk}^{\mathrm{R}} y_{pfr} \\
&- \sum_{b\in\mathcal{B}}\sum_{k\in\mathcal{K}^{\mathrm{S}}}\sum_{c\in C^{\mathrm{S}}} \Psi_{fbk}^{\mathrm{B}} M_k n_{pfkc,\mathrm{SLAG}} - \sum_{k\in\mathcal{K}^{\mathrm{G}}}\sum_{c\in C^{\mathrm{O}}\setminus\{18\}} M_k n_{pfkc,\mathrm{RSRED}} \\
&- m_{pf} - u_{pf} - q_{pf} = 0 \qquad p \in \mathcal{P},\ f \in \mathcal{F}_p \quad (10)
\end{aligned}$$

$$x_{pb}^{\mathrm{B}} = \sum_{f\in\mathcal{F}_p}\sum_{r\in\mathcal{R}}\sum_{k\in\mathcal{K}} \Psi_{fbk}^{\mathrm{B}} \Psi_{rk}^{\mathrm{R}} y_{pfr} + \sum_{f\in\mathcal{F}_p}\sum_{k\in\mathcal{K}^{\mathrm{S}}}\sum_{c\in C^{\mathrm{S}}} \Psi_{fbk}^{\mathrm{B}} M_k n_{pfkcv} \qquad p \in \mathcal{P},\ b \in \mathcal{B},\ v \in \{\mathrm{SLAG}\} \quad (11)$$

Constraints (8) restrict the feed of raw materials and slag to a furnace to within the capacity of the furnace. Constraints (9) handle the reuse of undersized lumps relative to the feed of other resources used in a furnace.

Constraints (10) handle the mass balance in a furnace. The constraints include the mass of the modelled elements and oxides fed to the furnace, the mass of the slag fed to the furnace, the mass of oxygen accounted for twice due to the modelling of CO_2 entering the Boudouard reaction, the mass of CO taking part in the prereduction in the furnace, less the mass of the furnace by-products from the raw material feed and slag feed, the mass of CO and CO_2 off-gas emissions, the metal output to either the MOR or LC SiMn refining and crushing processes and the mass of produced slag. For HC FeMn furnaces, the slag terms $n_{pfkc,\mathrm{SLAG}}$ are zero as no slag is sent to an HC FeMn furnace. For MC SiMn furnaces, the produced slag terms q_{pf} are zero as the slag is assumed to be a discard slag. The term $\sum_{k\in\mathcal{K}^{\mathrm{G}}}\sum_{c\in C^{\mathrm{O}}\setminus\{18\}} M_k n_{pfkc,\mathrm{RSRED}}$ excludes chemical reaction 18, which is the Boudouard reaction, because it uses the same variable name, but it accounts for the off-gases leaving the furnace, not the re-entering gas.

Constraints (11) state the relationship between the total feed of raw materials and slag sent to the furnaces and the amount of a discardable by-product produced by the furnaces at a plant. The constraints for electrical power

ACCEPTED MANUSCRIPT

ACCEPTED MANUSCRIPT

consumption follows the given thermodynamic relations. They have the same structure as (10) using coefficients for formation and sensible enthalpies for the furnace temperature. These constraints are omitted for readability.

Furnace-Slag Connection Constraints

$$\phi_{pfk} q_{pf} = M_k \sum_{c \in \mathcal{C}^{\mathrm{S}}} B_{fkc} \alpha_{pfkc} \qquad p \in \mathcal{P},\ f \in \mathcal{F}_p^{\mathrm{FeMn}},\ k \in \mathcal{K}^{\mathrm{S}} \quad (12)$$

$$\sum_{g \in \mathcal{P}} \sum_{t \in \mathcal{F}_g^{\mathrm{SiMn}}} \sigma_{pfgt} \leq q_{pf} \qquad p \in \mathcal{P},\ f \in \mathcal{F}_p^{\mathrm{FeMn}} \quad (13)$$

$$\sum_{p \in \mathcal{P}} \sum_{f \in \mathcal{F}_p^{\mathrm{FeMn}}} \phi_{pfk} \sigma_{pfgt} = M_k \sum_{c \in \mathcal{C}^{\mathrm{S}}} n_{gtkcv} \qquad g \in \mathcal{P},\ t \in \mathcal{F}_g^{\mathrm{SiMn}},\ k \in \mathcal{K}^{\mathrm{S}},\ v \in \{\mathrm{SLAG}\} \quad (14)$$

$$\overline{\Phi}_k \geq \phi_{pfk} \geq \underline{\Phi}_k \qquad p \in \mathcal{P},\ f \in \mathcal{F}_p^{\mathrm{FeMn}},\ k \in \mathcal{K}^{\mathrm{S}} \quad (15)$$

$$\sum_{k \in \mathcal{K}^{\mathrm{S}}} \phi_{pfk} = 1 \qquad p \in \mathcal{P},\ f \in \mathcal{F}_p^{\mathrm{FeMn}} \quad (16)$$

$$\overline{\Lambda}(m_{pf} + u_{pf}) \geq q_{pf} \geq \underline{\Lambda}(m_{pf} + u_{pf}) \qquad p \in \mathcal{P},\ f \in \mathcal{F}_p^{\mathrm{FeMn}} \quad (17)$$

Constraints (12) couple the produced amount of slag q_{pf} in an HC FeMn furnace and its constituent fractions ϕ_{pfk}, to the mass of the constituents $M_k \alpha_{pfkc}$ pulled from the chemical reactions occurring in the HC FeMn furnace. Thus, the mass of element or oxide k in the slag extracted from an HC FeMn furnace equals the amount of mass of element or oxide k removed from the redox reactions in the furnace. The left-hand side terms of the constraints are nonlinear and, therefore, complicates the problem. The constraints are unique to this problem because there are no pooling problems in the manganese alloy industry, to the authors' knowledge, that extracts a proportion of a specific constituent from a blending process. The closest similarities may be found in the separation processes in the crude oil industry.

Constraints (13) state that sending slag to MC SiMn furnaces from an HC FeMn furnace is optional, by allowing less than the produced slag to be sent. This allows the slag to be discarded if it is unfavourable to feed it to MC SiMn furnaces. The slag transportation and slag feed to an MC SiMn furnace are coupled by constraints (14). These are nonlinear terms common to the pooling problem. Constraints (15) induce lower and upper bounds on the slag compostition. Constraints (16) enforce that the sum of the weight percentages of all the slag constituents must make up the total slag content. Constraints (17) ensure that it is always produced at least a minimum amount of slag in a HC FeMn furnace relative to the metal produced and set the upper bound on the slag production relative to the metal production.

MOR Constraints

$$\sum_{f \in \mathcal{F}_p^{\mathrm{FeMn}}} m_{pf} + o_p + c_p \leq Q_p^{\mathrm{MOR}} \qquad p \in \mathcal{P} \quad (18)$$

ACCEPTED MANUSCRIPT

$$\sum_{f \in \mathcal{F}_p^{\text{FeMn}}} m_{pf} + o_p + c_p \; - x_{pe}^{\text{E}} - \sum_{b \in \mathcal{B}'} x_{pb}^{\text{B}} = \; 0 \qquad p \in \mathcal{P}, \;\; \mathcal{B}' = \{\text{MOR dust, MC FeMn}\} \;\; (19)$$

$$o_p \;\; = \;\; \Omega^{\text{MOR}} \sum_{f \in \mathcal{F}_p^{\text{FeMn}}} m_{pf} \qquad p \in \mathcal{P} \;\; (20)$$

$$c_p \;\; \leq \;\; \Psi^{\text{MFeL}} \sum_{f \in \mathcal{F}_p^{\text{FeMn}}} m_{pf} \qquad p \in \mathcal{P} \;\; (21)$$

$$x_{pb}^{\text{B}} \;\; = \;\; \Psi_b^{\text{MOR}} \Big(\sum_{f \in \mathcal{F}_p^{\text{FeMn}}} m_{pf} + o_p \Big) \qquad p \in \mathcal{P}, \;\; b \in \{\text{MOR dust}\} \;\; (22)$$

Constraints (18) ensure that the feed of HC FeMn, oxygen, and undersized lumps added to the MOR do not surpass the MOR capacity. Constraints (19) handle the mass balance in the MOR. Constraints (20) state that the oxygen used in the MOR equals a fixed ratio of the added HC FeMn. By calculating this ratio, there is no need to include a chemical reaction in the model. Constraints (21) set the upper bound on how much MC FeMn undersized lumps it is possible to add to the MOR relative to the feed of metal. This is to prevent too low temperatures in the MOR. Constraints (22) state that a certain percentage of the mass fed to the MOR ends up as saleable MOR dust.

LC SiMn Refining Station Constraints

$$\sum_{f \in \mathcal{F}_p^{\text{SiMn}}} m_{pf} + s_p + a_p \;\; \leq \;\; Q_p^{\text{REF}} \qquad p \in \mathcal{P} \;\; (23)$$

$$\sum_{f \in \mathcal{F}_p^{\text{SiMn}}} m_{pf} + s_p + a_p - h_p \;\; = \;\; 0 \qquad p \in \mathcal{P} \;\; (24)$$

$$s_p \;\; = \;\; \Omega^{\text{REF}} \sum_{f \in \mathcal{F}_p^{\text{SiMn}}} m_{pf} \qquad p \in \mathcal{P} \;\; (25)$$

$$a_p \;\; \leq \;\; \Psi^{\text{LSiL}} \Big(\sum_{f \in \mathcal{F}_p^{\text{SiMn}}} m_{pf} + s_p \Big) \qquad p \in \mathcal{P} \;\; (26)$$

Constraints (23) handle the capacity of an LC SiMn refining station. The mass balance in the LC SiMn refining station is handled by constraints (24). Constraints (25) relate the total amount of silicon waste needed to add, relative to the amount of MC SiMn, to alter the product composition. The constraints ensure that it is not possible to get LC SiMn out from the refining process without mixing the correct amount of Si with the incoming feed of MC SiMn. The upper limit on how much LC SiMn undersized lumps it is possible to add to the LC SiMn refining station process is given by constraints (26).

Crushing Constraints

$$\sum_{f \in \mathcal{F}_p^{\text{FeMn}}} u_{pf} \;\; = \;\; x_{pe}^{\text{E}} + x_{pb}^{\text{B}} \qquad p \in \mathcal{P}, \;\; e \in \{\text{HC FeMn}\}, \;\; b \in \{\text{HC FeMn}\} \;\; (27)$$

ACCEPTED MANUSCRIPT

$$x^{\mathrm{B}}_{pb} = \Psi^{\mathrm{CRUSH}}_{b}(x^{\mathrm{E}}_{pe} + x^{\mathrm{B}}_{pb}) \qquad p \in \mathcal{P},\ b \in \{\text{MC FeMn}\} \quad (28)$$

$$\sum_{f \in \mathcal{F}_p} y_{pfr} \leq x^{\mathrm{B}}_{pb} \qquad p \in \mathcal{P}, r \in \{\text{HC FeMn, MC SiMn}\}, b \in \{\text{HC FeMn, MC SiMn}\} \quad (29)$$

$$c_p \leq x^{\mathrm{B}}_{pb} \qquad p \in \mathcal{P},\ b \in \{\text{MC FeMn}\} \quad (30)$$

$$a_p \leq x^{\mathrm{B}}_{pb} \qquad p \in \mathcal{P},\ b \in \{\text{LC SiMn}\} \quad (31)$$

Constraints (27) ensure that the total amount of HC FeMn alloy from a plant's HC FeMn furnaces sent directly to crushing equals the HC FeMn end-product and by-products produced at the plant. Constraints (28) ensure that a given percentage of the alloy that flows from the HC FeMn furnaces and the MOR ends up as undersized lumps. Similar constraints exist for the SiMn production for constraints (27) - (28). To have a sustainable consumption of undersized lumps, the volume of undersized lumps used in the process should be less than or equal to the volume of undersized lumps exiting the crushing process. Constraints (29) - (31) ensure that this condition is satisfied. Constraints (29) allow both HC FeMn and MC SiMn undersized lumps to be used in both furnace types.

Final Inventory and Demand Constraints

$$g^{\mathrm{F}}_{e} = D^{\mathrm{F}}_{e} \qquad e \in \mathcal{E} \quad (32)$$

$$g^{\mathrm{O}}_{e} \leq D^{\mathrm{O}}_{e} \qquad e \in \mathcal{E} \quad (33)$$

Constraints (32) handle the demand from fixed contracts while constraints (33) handle the limit on the spot market.

Chemical Balance Constraints

$$\sum_{c \in \mathcal{C}} T_{kcv} n_{pfkcv} = \frac{1 - \sum_{b \in \mathcal{B}} \Psi^{\mathrm{B}}_{fbk}}{M_k} \sum_{r \in \mathcal{R}} \Psi^{\mathrm{R}}_{rk} y_{pfr} \qquad p \in \mathcal{P},\ f \in \mathcal{F}_p,\ k \in \mathcal{K},\ v \in \{\text{FED}\} \quad (34)$$

$$\sum_{v \in \mathcal{V} \setminus \{\text{SLAG}\}} \sum_{k \in \mathcal{K}} A_{fkcv} n_{pfkcv} + \sum_{k \in \mathcal{K}^{\mathrm{S}}} (1 - \sum_{b \in \mathcal{B}} \Psi^{\mathrm{B}}_{fbk}) A_{fkc,\mathrm{SLAG}} n_{pfkc,\mathrm{SLAG}}$$
$$- \sum_{k \in \mathcal{K}} B_{fkc} \alpha_{pfkc} = 0 \qquad p \in \mathcal{P},\ f \in \mathcal{F}_p,\ c \in C^{\mathrm{O}} \quad (35)$$

$$\sum_{v \in \mathcal{V} \setminus \{\text{SLAG}\}} \sum_{k \in \mathcal{K}} A^{\mathrm{LS}}_{fkcv} n_{pfkcv} + \sum_{k \in \mathcal{K}^{\mathrm{S}}} (1 - \sum_{b \in \mathcal{B}} \Psi^{\mathrm{B}}_{fbk}) A^{\mathrm{LS}}_{fkc,\mathrm{SLAG}} n_{pfkc,\mathrm{SLAG}}$$
$$- \sum_{k \in \mathcal{K}} B_{fkc} \alpha_{pfkc} = 0 \qquad p \in \mathcal{P},\ f \in \mathcal{F}_p,\ c \in C^{\mathrm{O}} \quad (36)$$

$$\sum_{v \in \mathcal{V}} \sum_{k \in \mathcal{K}} A^{\mathrm{RS}}_{fkcv} n_{pfkcv} = 0 \qquad p \in \mathcal{P},\ f \in \mathcal{F}_p,\ c \in C^{\mathrm{O}} \quad (37)$$

$$\sum_{v \in \mathcal{V}} \sum_{k \in \mathcal{K}} A_{fkcv} n_{pfkcv} = 0 \qquad p \in \mathcal{P},\ f \in \mathcal{F}_p,\ c \in C^{\mathrm{C}} \quad (38)$$

ACCEPTED MANUSCRIPT

$$n_{pfk,c+1,\mathrm{RED}} = n_{pfkc,\mathrm{RSRED}} \qquad p \in \mathcal{P},\ f \in \mathcal{F}_p,\ k \in \{\mathrm{Mn_2O_3},\ \mathrm{Mn_3O_4},\ \mathrm{MnO}\ ,\ \mathrm{Fe_2O_3}\ \mathrm{Fe_2O_3},\ \mathrm{Fe_3O_4},\ \mathrm{FeO}\},\ c \in \{1,2,3,6,7\} \quad (39)$$

Constraints (34) connect the chemical processes in a furnace to the raw material feed. The left-hand side of the constraints states that the total amount of moles of an element or oxide k used in the chemical reactions in each furnace has to equal the feed of that element or oxide to the furnace. The parameters T_{kcv} ensure that n_{pfkcv} cannot take any other value than zero where element or oxide $k \in \mathcal{K}$ is not present in chemical reaction c for variable $v \in \{\mathrm{FED}\}$. The right-hand side of the constraints multiplies the weight percentage for each element or oxide k in raw material r with the total weight of the raw material to find the weight of the element or oxide in the raw material. The sum is taken over all raw materials so that the total feed of the respective element or oxide is found. It is then divided by molar mass in mole per tonne to determine the amount of mole fed to the furnace for element or oxide k. The term $(1 - \sum_{b \in \mathcal{B}} \Psi^{\mathrm{B}}_{fbk})$ removes the amount of moles that ends up as discardable by-products from the feed since the chemical reactions do not account for the production of these.

The general form of the chemical reactions is given by constraints (35) - (37). The constraints enforce that the mole balances equal zero. Each chemical reaction is represented by three constraints to ensure the correct relationships between reactants and resultants. Constraints (35) represent the complete chemical reaction, while constraints (36) ensure correct ratios between the reactants, and constraints (37) the resultants.

The output of Mn, Fe, Si, and C from the redox reactions and the direct feed of the respective elements from ores and undersized lumps are added together in constraints (38) to find the total mass of each element in the furnace output alloy. The reactants in some of the chemical reactions originate from a resultant in the previous reaction, therefore the $n_{pfk,c+1,\mathrm{RED}}$ variables in these chemical reactions equals the $n_{pfkc,\mathrm{RSRED}}$ in the previous reaction. This is handled by constraints (39).

An example of the application of constraints (35) - (37) to model chemical reaction (71), $3\,\mathrm{Mn_2O_3(s)} + \mathrm{CO\ (g)} \longrightarrow 2\,\mathrm{Mn_3O_4(s)} + \mathrm{CO_2(g)}$, is provided in equations (40a) - (40c).

$$2n_{pf,\mathrm{Mn_2O_3},2,\mathrm{FED}} + 2n_{pf,\mathrm{Mn_2O_3},2,\mathrm{RED}} + 6n_{pf,\mathrm{CO},2,\mathrm{FED}} - 3n_{pf,\mathrm{Mn_3O_4},2,\mathrm{RSRED}} - 6n_{pf,\mathrm{CO_2},2,\mathrm{RSRED}} = 0 \qquad p \in \mathcal{P},\ f \in \mathcal{F}_p \quad (40a)$$

$$n_{pf,\mathrm{Mn_2O_3},2,\mathrm{FED}} + n_{pf,\mathrm{Mn_2O_3},2,\mathrm{RED}} - 3n_{pf,\mathrm{CO},2,\mathrm{FED}} = 0 \qquad p \in \mathcal{P},\ f \in \mathcal{F}_p \quad (40b)$$

$$n_{pf,\mathrm{Mn_3O_4},2,\mathrm{RSRED}} - 2n_{pf,\mathrm{CO_2},2,\mathrm{RSRED}} = 0 \qquad p \in \mathcal{P},\ f \in \mathcal{F}_p \quad (40c)$$

Equation (40a) is the representation of reaction (71) with the correct mole ratios between the reactants and resultants. Equation (40b) and equation (40c) balance the reactants and the resultants, respectively.

ACCEPTED MANUSCRIPT

Boudouard Reaction Constraints

$$n_{pf,\mathrm{C},18,\mathrm{FED}} + n_{pf,\mathrm{CO_2},18,\mathrm{TOT}} - n_{pf,\mathrm{CO},18,\mathrm{RSRED}} = 0 \qquad p \in \mathcal{P},\ f \in \mathcal{F}_p \quad (41a)$$

$$n_{pf,\mathrm{C},18,\mathrm{FED}} - n_{pf,\mathrm{CO_2},18,\mathrm{TOT}} = 0 \qquad p \in \mathcal{P},\ f \in \mathcal{F}_p \quad (41b)$$

$$n_{pf,\mathrm{CO_2},18,\mathrm{TOT}} = (1-\Upsilon) \sum_{c \in C \setminus \{1,2\}} n_{pf,\mathrm{CO_2},c,\mathrm{RSRED}} \qquad p \in \mathcal{P},\ f \in \mathcal{F}_p \quad (41c)$$

$$\sum_{c \in C^{\mathrm{O}}} n_{pf,\mathrm{CO},c,\mathrm{TOT}} \leq n_{pf,\mathrm{CO},18,\mathrm{RSRED}} + \sum_{c \in C^{\mathrm{S}}} n_{pf,\mathrm{CO},c,\mathrm{RSRED}} \qquad p \in \mathcal{P},\ f \in \mathcal{F}_p \quad (41d)$$

Constraints (41a) are the Boudouard reaction given in reaction (79). Constraints (41b) ensure correct ratio between the left side reactants, no constraints are needed for the right side ratio as only one resultant exists. Constraints (41c) handle the degree of pre-reduction in the furnace, i.e. how much CO_2 that is consumed by the Boudouard reaction. Following the given definition of pre-reduction, the term has to be formulated as $(1-\Upsilon)$ to model the amount of CO_2 re-entering the process correctly. The chemical reactions involving MnO_2 and Mn_2O_3 are not normally involved in prereduction and are therefore not included in the sum of the right side term. Constraints (41d) ensure that the total CO fed to reactions (70) - (72) and (75) - (76) is less than or equal to the CO resulting from the Boudouard reaction and the reactions (73), (77), and (78). The CO and CO_2 that do not re-enter the process are released as off-gases.

Chemical Content Constraints

$$M_k \sum_{c \in C^{\mathrm{C}}} T_{kcv} n_{pfkcv} = \Psi_k^{\mathrm{FeMn}} (m_{pf} + u_{pf}) \qquad p \in \mathcal{P},\ f \in \mathcal{F}_p^{\mathrm{FeMn}},\ k \in \mathcal{K}^{\mathrm{C}},\ v \in \{\mathrm{TOT}\} \quad (42)$$

$$M_k \sum_{c \in C^{\mathrm{C}}} T_{kcv} n_{pfkcv} = \Psi_k^{\mathrm{SiMn}} (m_{pf} + u_{pf}) \qquad p \in \mathcal{P},\ f \in \mathcal{F}_p^{\mathrm{SiMn}},\ k \in \mathcal{K}^{\mathrm{C}},\ v \in \{\mathrm{TOT}\} \quad (43)$$

Constraints (42) and (43) ensure that the required content of critical elements is satisfied in the HC FeMn and the MC SiMn furnace, respectively.

Non-negativity Constraints

$$a_p, c_p, h_p, o_p, s_p \geq 0 \qquad p \in \mathcal{P} \quad (44)$$

$$g_e^{\mathrm{F}}, g_e^{\mathrm{O}} \geq 0 \qquad e \in \mathcal{E} \quad (45)$$

$$x_{pb}^{\mathrm{B}} \geq 0 \qquad p \in \mathcal{P},\ b \in \mathcal{B} \quad (46)$$

$$x_{pe}^{\mathrm{E}} \geq 0 \qquad p \in \mathcal{P},\ e \in \mathcal{E} \quad (47)$$

$$e_{pf}, m_{pf}, q_{pf}, u_{pf} \geq 0 \qquad p \in \mathcal{P},\ f \in \mathcal{F}_p \quad (48)$$

$$\phi_{pfk} \geq 0 \qquad p \in \mathcal{P},\ f \in \mathcal{F}_p,\ k \in \mathcal{K}^{\mathrm{S}} \quad (49)$$

$$y_{pfr} \geq 0 \qquad p \in \mathcal{P},\ f \in \mathcal{F}_p,\ r \in \mathcal{R} \quad (50)$$

ACCEPTED MANUSCRIPT

$$\sigma_{pfgt} \geq 0 \qquad p \in \mathcal{P},\ f \in \mathcal{F}_p,\ g \in \mathcal{P},\ t \in \mathcal{F}_g \quad (51)$$

$$\alpha_{pfkc} \geq 0 \qquad p \in \mathcal{P},\ f \in \mathcal{F}_p,\ k \in \mathcal{K},\ c \in \mathcal{C} \quad (52)$$

$$n_{pfkcv} \geq 0 \qquad p \in \mathcal{P},\ f \in \mathcal{F}_p,\ k \in \mathcal{K},\ c \in \mathcal{C},\ v \in \mathcal{V} \quad (53)$$

4. Solution by the Multiparametric Disaggregation Technique

The model has bilinear terms to model mixing of the slag quality components and is, therefore, a nonconvex NLP. We have used the Multiparametric Disaggregation Technique (MDT), Teles et al. (2012, 2013); Kolodziej et al. (2013a,b), to formulate the bilinear terms in the MAMP problem as systems of linear inequalities. In the MDT, a lower bound problem (LBP) and an upper bound problem (UBP) are derived. The LBP and UBP can then be solved by standard MILP solvers with increasing accuracy until the global optimality gap ε is satisfactory. To parameterise and discretise the bilinear constraints, new sets, parameters, and variables are defined. These are found in Tables 4 - 6, respectively.

Table 4: Definition of sets for the MDT

Set	
$\mathcal{M}$	Set of single digit integers, $(0-9)$, indexed by m
$\mathcal{L}$	Set of negative integers, indexed by l

Table 5: Definition of parameters for the MDT

Parameter	
j	The last significant number's position.
$\underline{q}_{pf}$	Lower bound on the slag produced by furnace f at plant p.
$\overline{q}_{pf}$	Upper bound on the slag produced by furnace f at plant p.
ε	Optimality gap between the lower bound problem objective value and the best bound of the upper bound problem.

Table 6: Definition of variables for the MDT

Variable	
$\hat{q}_{pfkml}$	The disaggregated flow variables of the product $q_{pf}\mu_{pfkml}$.
μ_{pfkml}	1 if the decimal power l is active for integer m for element or oxide k in furnace f at plant p, 0 otherwise.
λ_{pfkl}	Discretisation variable for use in reformulating ϕ_{pfk}.
$\Delta\phi_{pfk}$	Slack variable for the continuous representation of the discretised variable ϕ_{pfk}.

4.1. Lower Bound Problem

This section describes how the bilinear constraints (12) are formulated as a system of linear constraints in the LBP. Of the two variables appearing in a bilinear term, one variable is parameterised and the other disaggregated (Teles

ACCEPTED MANUSCRIPT

et al., 2012). A continuous variable can be disaggregated into a set of non-negative continuous variables, which can only assume positive values up to the upper bound of the original variable, (Teles et al., 2013). The ϕ_{pfk} variables are chosen to be parameterised since they are limited between zero and one. This reduces the feasible region of the problem compared with disaggregating ϕ_{pfk} and parameterising the variables q_{pf} instead, which have a range between zero and the maximum slag production possible in a furnace. The reformulation of constraints (12) is based on the MDT found in *Kolodziej et al. (2013a)* and yields the following constraints:

$$\phi_{pfk} q_{pf} = \sum_{l \in \mathcal{L}} \sum_{m \in \mathcal{M}} 10^l m \cdot \hat{q}_{pfkml} \qquad p \in \mathcal{P},\ f \in \mathcal{F}_p^{\text{FeMn}},\ k \in \mathcal{K}^{\text{S}} \quad (54)$$

$$\phi_{pfk} = \sum_{l \in \mathcal{L}} \sum_{m \in \mathcal{M}} 10^l m \cdot \mu_{pfkml} \qquad p \in \mathcal{P},\ f \in \mathcal{F}_p^{\text{FeMn}},\ k \in \mathcal{K}^{\text{S}} \quad (55)$$

$$q_{pfk} = \sum_{m \in \mathcal{M}} \hat{q}_{pfkml} \qquad p \in \mathcal{P},\ f \in \mathcal{F}_p^{\text{FeMn}},\ k \in \mathcal{K}^{\text{S}},\ l \in \mathcal{L} \quad (56)$$

$$\overline{q}_{pf} \mu_{pfkml} \geq \hat{q}_{pfkml} \geq \underline{q}_{pf} \mu_{pfkml} \qquad p \in \mathcal{P},\ f \in \mathcal{F}_p^{\text{FeMn}},\ k \in \mathcal{K}^{\text{S}},\ m \in M,\ l \in \mathcal{L} \quad (57)$$

$$\sum_{m \in \mathcal{M}} \mu_{pfkml} = 1 \qquad p \in \mathcal{P},\ f \in \mathcal{F}_p^{\text{FeMn}}, k \in \mathcal{K}^{\text{S}},\ l \in \mathcal{L} \quad (58)$$

$$\mu_{pfkml} \in \{0, 1\} \qquad p \in \mathcal{P},\ f \in \mathcal{F}_p^{\text{FeMn}},\ k \in \mathcal{K}^{\text{S}},\ m \in M,\ l \in \mathcal{L} \quad (59)$$

In constraints (54), the bilinear term $\phi_{pfk} q_{pf}$ is replaced by a weighted sum of continuous variables. Constraints (55) parameterise the variable ϕ_{pfk} as a sum of binary variables where $\mu_{pfkml} = 1$ if the l^{th} decimal place contains the number m, i.e $\phi_{pfk} = 0.43 \rightarrow \mu_{pfk4,-1} = 1, \mu_{pfk3,-2} = 1$. In constraints (56), the other variable in the bilinear expression is connected to the new continuous variables, which are bounded in constraints (57). Constraints (58) are convexity constraints and constraints (59) are variable restrictions. Constraints (14) are reformulated in the same manner. Implementing the reformulations of constraints (12) and (14) in the MAMP problem yields the LBP.

4.2. Upper Bound Problem

This section describes the reformulation of constraints (12) for the UBP. The same derivation as found in Kolodziej et al. (2013a) is used, leading to a continuous representation of the discretised variables. The result is the following constraints, which replaces constraints (12):

$$\phi_{pfk} q_{pf} = \sum_{l \in \mathcal{L}} \sum_{m \in \mathcal{M}} 10^l m \cdot \hat{q}_{pfkml} + \Delta\phi_{pfk} q_{pf} \qquad p \in \mathcal{P},\ f \in \mathcal{F}_p^{\text{FeMn}},\ k \in \mathcal{K}^{\text{S}} \quad (60)$$

$$\phi_{pfk} = \sum_{l \in \mathcal{L}} \sum_{m \in \mathcal{M}} 10^l m \cdot \mu_{pfkml} + \Delta\phi_{pfk} \qquad p \in \mathcal{P},\ f \in \mathcal{F}_p^{\text{FeMn}},\ k \in \mathcal{K}^{\text{S}} \quad (61)$$

$$q_{pf} = \sum_{m \in \mathcal{M}} \hat{q}_{pfkml} \qquad p \in \mathcal{P},\ f \in \mathcal{F}_p^{\text{FeMn}},\ k \in \mathcal{K}^{\text{S}},\ l \in \mathcal{L} \quad (62)$$

$$\overline{q}_{pf} \mu_{pfkml} \geq \hat{q}_{pfkml} \geq \underline{q}_{pf} \mu_{pfkml} \qquad p \in \mathcal{P},\ f \in \mathcal{F}_p^{\text{FeMn}},\ k \in \mathcal{K}^{\text{S}},\ m \in M,\ l \in \mathcal{L} \quad (63)$$

$$\sum_{m \in \mathcal{M}} \mu_{pfkml} = 1 \qquad p \in \mathcal{P},\ f \in \mathcal{F}_p^{\text{FeMn}},\ k \in \mathcal{K}^{\text{S}},\ l \in \mathcal{L} \quad (64)$$

ACCEPTED MANUSCRIPT

$$\mu_{pfkml} \in \{0,1\} \qquad p \in \mathcal{P},\ f \in \mathcal{F}_p^{\text{FeMn}},\ k \in \mathcal{K}^{\text{S}},\ m \in M,\ l \in \mathcal{L} \quad (65)$$

$$\overline{q}_{pf}\Delta\phi_{pfk} \geq \Delta\phi_{pfk}q_{pf} \geq \underline{q}_{pf}\Delta\phi_{pfk} \qquad p \in \mathcal{P},\ f \in \mathcal{F}_p^{\text{FeMn}},\ k \in \mathcal{K}^{\text{S}} \quad (66)$$

$$\Delta\phi_{pfk}q_{pf} \geq (q_{pf} - \overline{q}_{pf})10^j + \overline{q}_{pf}\Delta\phi_{pfk} \qquad p \in \mathcal{P},\ f \in \mathcal{F}_p^{\text{FeMn}},\ k \in \mathcal{K}^{\text{S}} \quad (67)$$

$$\Delta\phi_{pfk}q_{pf} \leq (q_{pf} - \underline{q}_{pf})10^j + \underline{q}_{pf}\Delta\phi_{pfk} \qquad p \in \mathcal{P},\ f \in \mathcal{F}_p^{\text{FeMn}},\ k \in \mathcal{K}^{\text{S}} \quad (68)$$

$$10^j \geq \Delta\phi_{pfk} \geq 0 \qquad p \in \mathcal{P},\ f \in \mathcal{F}_p^{\text{FeMn}},\ k \in \mathcal{K}^{\text{S}} \quad (69)$$

The structure of this reformulation is the same as in the LBP, but a slack variable is added to the discretisation. This relaxes the problem and gives an upper bound on the optimal objective value. Constraints (14) are reformulated in the same manner for the UBP. Implementing the reformulations of constraints (12) and (14) in the MAMP problem, yields the UBP.

5. Computational Study

We have evaluated the applicability and limitations of the MAMP through a computational study. First, the test case is presented, based on data provided by Eramet Norway, before testing the applicability of the MDT technique presented in Section 4. Further, we compare the results of applying the model described in Section 3, with today's operational practice. Finally, we investigate how the slag composition, and the slag-to-metal ratio, changes with increasing demand for all products.

The mathematical model is written in the algebraic modelling language Mosel and run in FICO® Xpress Optimisation Suite 7.9 using an HP bl685c G7 computer with an 2.2GHz AMD Opteron 6274 16 core CPU and 128 GB RAM on a Linux operation system.

5.1. Test Case

The test case used in this computational study is based on the production set-up and data provided by Eramet Norway, supplemented by data found in the literature. Eramet Norway operates seven furnaces distributed across three plants, where three are HC FeMn furnaces and four are MC SiMn furnaces. Plant 1 has one HC FeMn furnace and one MC SiMn furnace, Plant 2 has three MC SiMn furnaces, and Plant 3 has two HC FeMn furnaces.

All furnaces are set to have 22% pre-reduction, as used in *Olsen et al. (2007)*, thus $\Upsilon = 0.22$. Each furnace lose 35% of the heat generated to the surroundings, thus $L^{\text{H}} = 1.35$. The electricity price is set lower than the current market price, as alloy companies often have lucrative price agreements. The electricity price is, therefore, set to $C^{\text{E}} = 0.0118$ USD/kWh. The input mass and electrical power capacity of each furnace are set to 1000 tonnes/40 MW and 750 tonnes/30 MW for HC FeMn and MC SiMn furnaces, respectively. In practice, it is usually the electrical power that limits furnace capacity. The refining processes' input capacities are set sufficiently high not to be limiting factors. The feed limit for each type of undersized lump is given as a weight fraction of the raw material feed to the furnaces, or the liquid metal feed to the MORs and LC SiMn refining stations. The feed limit fractions are set to 0.10.

ACCEPTED MANUSCRIPT

The demands and revenues for fixed and spot contracts per production period can be found in Table 7. It is assumed that the total market demand is greater than the total furnace capacity. The production is thus limited by the mass and electrical power capacity of the furnaces. Estimated slag transportation costs between plants are set to 8.4 USD/tonne between Plant 1 and Plant 2, 14.0 USD/tonne between Plant 1 and Plant 3 and, 4.2 USD/tonne between Plant 2 and Plant 3. The production period is set to $\Delta T = 30$ days. It should be noted that the cost and revenue data provided by Eramet Norway are perturbed for confidentiality purposes.

Table 7: End-products with demands and revenues for fixed and spot contracts. Demand and spot market limit are given in tonnes, revenue is given in USD/tonne.

End-product e	**Demand** D_e^{F}	**Revenue** R_e^{F}	**Spot market limit** D_e^{O}	**Revenue** R_e^{O}
HC FeMn	13500	771	6000	810
MC FeMn	15000	899	6000	944
MC SiMn	10500	783	6000	822
LC SiMn	12000	853	6000	896

Each end-product is produced to satisfy certain content specifications. Explicit specifications are only set for the contents of HC FeMn and MC SiMn as these products are made in the furnaces where chemical composition is modelled. The content specifications for HC FeMn are: 0.790 Mn, 0.136 Fe, 0.004 Si, and 0.070 C. The MC SiMn specifications are 0.712, 0.081, 0.192, and 0.015 for the same elements, respectively. Notice that the composition of each end-product sum up to one. Correct content specifications of MC FeMn and LC SiMn are given implicitly by predetermined parameters for the refining stations. The weight percentage of every other constituent in MC FeMn and LC SiMn changes proportionally to the reduction of carbon as a result of the altered composition.

The mass output of slag is in relation to the total output of metal in an HC FeMn furnace. The maximum slag-to-metal ratio is set to $\overline{\Lambda} = 1.00$ and the minimum value $\underline{\Lambda} = 0.50$. The slag exiting the HC FeMn furnaces has set quality specification intervals for oxides with metal-bearing capabilities. The upper and lower bound on the slag quality are defined by the parameters $\overline{\Phi}_k$ and $\underline{\Phi}_k$, respectively. $\overline{\Phi}_k$ is 0.50 for MnO, 0.02 for FeO, 0.35 for SiO_2, 0.20 for Al_2O_3 and MgO, and 0.30 for CaO. $\underline{\Phi}_k$ is 0.30, 0.00, 0.15, 0.10, 0.5, and 0.10 for the same oxides, respectively. The sum of the lower bounds on the slag composition $\underline{\Phi}_k$ means that this amount of the slag composition is predetermined. As in the base instance, 70% of the slag composition is already determined. 30% of the slag composition is then left for the MAMP problem to decide. The greater the sum of the upper bound on the slag composition $\overline{\Phi}_k$, the greater the number of possible combinations of oxides with which to fill the remaining 30% of the slag composition. At every stage of the production, except at the LC SiMn refining station, by-products are produced as a fixed amount of the total feed to the process stage. These values are set to 0.02 for by-products produced in HC FeMn furnaces and 0.10 in the MC SiMn furnaces. The oxides Al_2O_3, MgO, and CaO completely exit the MC SiMn furnace as slag and thus the associated by-product parameters are 1.00 for these. In the MOR, the by-product fraction is 0.08. Values are based on *Olsen et al.*

ACCEPTED MANUSCRIPT

(2007).

A set of 19 raw materials is at disposal at each plant. These raw materials contain various elements and oxides of different concentrations. Oxygen, silicon waste, MC FeMn undersized lumps, and LC SiMn undersized lumps, named refining resources, are separated from the raw materials since these feed other processes than the furnace process. The inventories of these raw materials are assumed to be large enough to satisfy any demand.

5.2. Testing the applicability of the MDT

To be able to test the scalability of the MDT, some additional test instances are created. For these instances, all the data is equal to the test case presented above, except for the number of plants and furnaces. We name each instance *PX-YFeZSi*, where X denote the number of plants, and Y and Z the number of HC FeMn and MC SiMn furnaces, respectively. The Base case is thus named *P3-3Fe4Si*, while we introduce three additional instances: *P1-1Fe1Si*, *P2-2Fe2Si* and *P5-5Fe5Si*.

In addition, we need to decide on the values of some of the parameters used in the MDT, based on the values given for the base case. The parameters $\overline{q}_{pf}$ greatly affect the run time as they set the solution space for the volume of slag produced for each furnace. $\overline{q}_{pf}$ should therefore be set as tight as possible to avoid a too large feasible region. The parameters are naturally limited by the total amount of slag a furnace can produce per day. They are easily scaled by multiplying with ΔT. For the defined HC FeMn furnace capacities, a suitable mathematical upper bound is set to $\overline{q}_{pf} = 500\Delta T$, to not be a limiting factor. The parameters $\underline{q}_{pf}$ are set to zero as the HC FeMn furnace possibly can produce zero output. A similar parameter is defined for constraints (14) through the MDT.

For each test instance, both the LBP and the UBP were run for a maximum of 7200 seconds. Both the LBP and UBP is first solved with a discretization of -2, and if this problem is solved to optimality the remaining time is used to solve the same problem with a discretization of -3. The results of these tests are presented in Table 8. For each test instance, the number of variables and constraints for each discretization, the optimal objective value, and the computing time of the LBP, and the optimality gap and computing time of the UBP, as well as the total computing time and global optimality gap ϵ for the test instances, are given. The value of ϵ is calculated as $\epsilon = (\overline{z}(UBP) - \underline{z}(LBP))/\underline{z}(LBP)$, where $\overline{z}(p)$ and $\underline{z}(p)$ is the dual and primal bound, respectively, from problem p.

As Table 8 shows, the number of variables and constraints grows rapidly with small increases in the number of furnaces. Adding a furnace adds a new set of chemical balance constraints and furnace restrictions to the problem. This increase in the number of variables and constraints make the larger problems much more difficult to solve, which can be seen by the time it takes to solve the UBP and LBP, and the deterioration of the UBP gap as well as ϵ. The base instance *P3-3Fe4Si* is solved to an $\epsilon = 2.49\%$ within the time limit. The applied precision has a significant effect on the required computational time. For larger instances, the -2 precision is never completed, and thus some problems are never solved with a precision of -3. Generally, the solution to the LBP problem is better and located faster than for the UBP. It is worth noting that the MAMP problem can find feasible solutions even for large instances such as *P5-5Fe5Si*, however, it is not possible to know exactly how good the solution is, due to the large value of ϵ.

ACCEPTED MANUSCRIPT

Table 8: Statistics from the computational experiments. For the instances that were solved for both precision levels, the data are given as $\{a, b\}$, where a and b are the values for precision of -2 and -3, respectively. For the other instances, the data obtained when solving the problem with a precision of -2 is presented. The objective value is given in thousands of USD, while the computing times are given in seconds.

	LBP				UBP		MAMP Main	
Instance	**# Variables**	**# Constraints**	**Objective value**	**Time**	**Gap**	**Time**	**Time**	ϵ
P1-1Fe1Si	{1167, 1347}	{17927, 18065}	5652	{1,9}	0.00 %	{1,6}	17	0.09 %
P2-2Fe2Si	{4202, 4802}	{70929, 71709}	20912	{1839, 5359}	0.72 %	7200	14409	1.21 %
P3-3Fe4Si	7985	125477	35383	7200	2.05 %	7200	14470	2.49 %
P5-5Fe5Si	13280	183102	52406	7200	5.96 %	7200	14405	6.76 %

5.3. Comparison of the MAMP to Single Furnace Optimisation

The current industry practice is to optimise the production for individual furnaces based on software and expert judgement made by metallurgists. This practice is denoted single furnace optimisation and is the practice of optimising the profit of each single furnace, and consequently the metal it produces, without regards to the overall production. This may be sub-optimal compared with planning the production when taking the multi-plant production into consideration. In this section we investigate if, and how, solving the MAMP problem can improve production planning.

To simulate single furnace optimisation, the following process is used. An instance only containing one HC FeMn furnace and an instance only containing one MC SiMn furnace are created. The authors assume that the single furnace optimisation process is done by satisfying the fixed contracts first, then the spot contracts with the highest profit. In the first iteration, the HC FeMn instance is solved with the total demand as input. The demand is then reduced with the production in the first iteration and the instance is solved again. This is done for three iterations with the HC FeMn instance, followed by four iterations with the MC SiMn instance. The results from the HC FeMn production iterations are shown in Table 9, together with the results from applying the MAMP formulation. It should be noted that the objective values for each furnace given for the MAMP problem is an approximation, since not all costs can easily be

ACCEPTED MANUSCRIPT

ACCEPTED MANUSCRIPT

allocated to a single furnace.

Table 9: Comparison of the MAMP formulation to single furnace optimisation for the FeMn production. Production volumes are given in tonnes. Objective values are given in thousand USD. * denotes that objective value is an approximation.

	Single Furnace Optimisation				**MAMP Optimisation**			
Plant p, Furnace f	**1, 1**	**3,6**	**3,7**	**Total**	**1, 1**	**3,6**	**3,7**	**Total**
Furnace Type	**FeMn**	**FeMn**	**FeMn**		**FeMn**	**FeMn**	**FeMn**	
u_{pf}, **to crushing**	0	8314	4175	12489	0	10688	3021	13709
m_{pf}, **to refining**	10439	2599	6519	19557	10998	0	8559	19557
q_{pf}, **produced slag**	5220	5456	5347	16023	5499	5344	5790	16633
x^{E}_{pe}, **HC FeMn**	0	7482	3758	11240	0	9620	2719	12339
x^{E}_{pe}, **MC FeMn**	9608	2392	6000	18000	10122	0	7878	18000
Obj. Val. FeMn	6668	5975	6741	19384	6967*	5225*	7092*	19284

The total demand of MC FeMn from fixed and spot contracts are satisfied for both production methods, while not all of the spot contract demand for HC FeMn is satisfied. This indicates that MC FeMn is the most profitable FeMn end-product. Considering only the production of FeMn alloys, the total profit of the single furnace optimization approach is actually better than the solution obtained from the MAMP problem. Even though the production of HC FeMn is lower, giving lower revenues, this is offset by cheaper raw materials. Thus, even though the slag-to-metal ratio is optimal at the lower bound of 0.50 in both production methods (can be verified by consulting $\frac{q_{pf}}{u_{pf}+m_{pf}}$), the amount and composition of the slag is different.

Figures 3 and 4 show the average slag composition of single furnace optimisation and MAMP optimisation, respectively. The most notable differences are the changes in the MnO, CaO, MgO, and Al_2O_3 concentrations. When optimising single HC FeMn furnaces, it is favourable to keep the MnO concentration in the slag to a minimum to maximise the HC FeMn output. Consequently, the oxides that are not substances of HC FeMn metal are maximised in the slag output. In MAMP optimisation, these concentrations are changed to optimise the overall production in the entire system. It is worth noting that even though the slag to metal ratio is at the lower bound also for the MAMP optimisation in this instance, it could increase the slag-to-metal ratio for an instance with different parameter settings, while the single furnace optimization always keeps the ratio at its lower bound.

ACCEPTED MANUSCRIPT

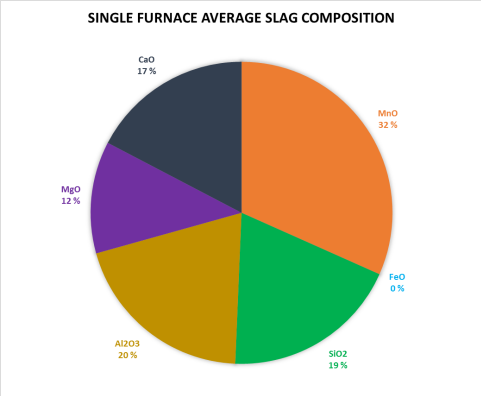

Figure 3: The average slag composition produced by the three HC FeMn furnaces using single furnace optimisation.

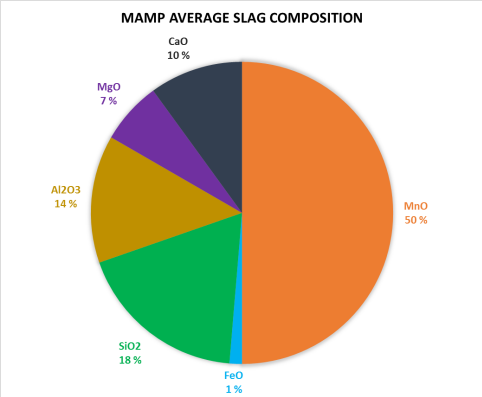

Figure 4: The average slag composition produced by the three HC FeMn furnaces using the MAMP formulation.

In the single furnace optimization we assume that the slag transportation between furnaces in the single furnace optimisation is based on minimising transportation costs, to make the two production planning methods as comparable as possible. This implies that as much slag as possible is sent internally at a plant if a plant has both HC FeMn and MC SiMn furnaces, as is the case at Plant 1. When the internal capacity of slag is reached, slag is transported to the plant with MC SiMn furnaces incurring the lowest transportation costs. The results from the single furnace optimisation method and the MAMP optimisation for the SiMn production are provided in Table 10.

All the produced slag is consumed in both production planning methods and all the LC SiMn demand is satisfied. The difference lies in the produced volume of MC SiMn, where an additional 673 tonnes of MC SiMn is produced by solving the MAMP problem due to different composition and allocation of the slag. This is an 8.52% increase in production of MC SiMn alloy. One can argue that the slag could have been distributed in another manner for the single furnace optimisation planning. However, regardless of what rule of thumb is used to distribute the slag it will be inferior to solving the MAMP problem which implicitly considers all possible ways of distributing it.

ACCEPTED MANUSCRIPT

ACCEPTED MANUSCRIPT

Table 10: Comparison of the MAMP problem to single furnace optimisation for the SiMn production and total profit. Production values are given in tonnes. Costs and objective values are given in thousand USD. *Cumulative Objective Value* is excluded the *Transportation Costs*. *Total profit* is the *Cumulative Objective Value* less the *Transportation Costs*. * denotes that objective value is an approximation.

	Single Furnace Optimisation					**MAMP Optimisation**				
Plant p, Furnace f	**1, 2**	**2,3**	**2,4**	**2,5**	**Total**	**1, 2**	**2,3**	**2,4**	**2,5**	**Total**
Furnace Type	**SiMn**	**SiMn**	**SiMn**	**SiMn**		**SiMn**	**SiMn**	**SiMn**	**SiMn**	
u_{pf}**, to crushing**	0	2786	5547	447	8780	2338	0	1381	5809	9528
m_{pf}**, to refining**	5021	2175	42	4755	11993	2856	5246	3892	0	11994
σ_{gtpf}**, used slag**	5220	5456	2674	2673	16023	5499	4095	3421	3618	16633
Leftover slag	0	0	0	0	0	0	0	0	0	0
x^{E}_{pe}**, MC SiMn**	0	2508	4992	402	7902	2104	0	1243	5228	8575
x^{E}_{pe}**, LC SiMn**	6280	2720	53	5947	15000	3571	6588	4841	0	15000
Obj. Val. SiMn	4418	3565	2929	4599	15511	3979*	4803*	4200*	3162*	16145
Cum. Obj. Val.					34895					35430
Transport. Costs	0	23	11	11	45	0	17	14	15	47
Discard Slag Cost					0					0
Total Profit					**34850**					**35383**

The solution to the MAMP problem yields more slag transportation than the single furnace optimisation, thus, transportation costs are greater. Using the MAMP formulation yields 1.53% higher profit compared to single furnace optimisation in the case of base instance *P3-3Fe4Si*. Two significant factors in making the MAMP formulation superior to single furnace optimisation are the volume of slag produced and the composition of the slag.

5.4. Optimal Slag Composition as a Function of Demand

The measure slag-to-metal ratio is widely used in the manganese alloy production industry. In the previous section, it can be observed that the slag-to-metal ratio is at the lower bound of 0.50 in all furnaces. The ratio has an upper limit of 1.00, i.e. one tonne slag is produced per tonne metal produced. We therefore investigate how this ratio changes with variations in the demand volume of the end-products. In this study we assume that the end-product demand is equal for all products, and distributed equally between FeMn and SiMn alloys. The fixed demand for all end-products are set as optional to make the solution to the MAMP problem select the most profitable ones. The end-product production volumes are also provided as it may better visualise the changes occurring in the slag-to-metal ratio and slag composition. The volumes produced of each end-product for increasing demand are illustrated in Figure 5.

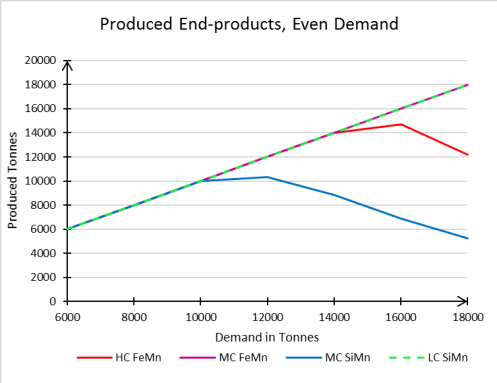

Figure 5: End-product production volumes for increasing demand when the demand is evenly distributed between FeMn and SiMn alloys.

Observe from Figure 5 that MC SiMn and HC FeMn are the first products in each production path to be reduced when reaching furnace capacities at 12 000 tonnes and 16 000 tonnes, respectively. The slight increase in productions before the steady decrease at the furnace capacities are due to the alteration of slag composition. A plot of the average slag-to-metal ratio as a function of demand is shown in Figure 6. A plot of the average slag composition as a function of demand is shown in Figure 7. Between 8 000 - 12 000 tonnes demand, a slight increase in slag-to-metal ratio can be observed. This is to better accommodate the lack of capacity in the furnace producing MC SiMn. At 12 000 tonnes, the HC FeMn furnace needs the capacity to produce more HC FeMn, and the slag-metal-ratio starts to decline. At 16 000 tonnes, it reaches the lower limit of the ratio and starts sending more of the metal output to MC FeMn refining, which is more profitable.

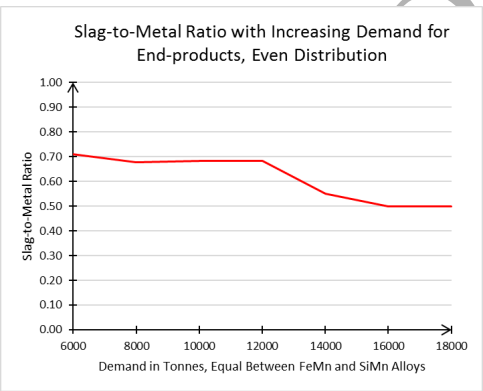

Figure 6: Average slag-to-metal ratio across all HC FeMn furnaces for increasing demand. Equal demand for each end-product.

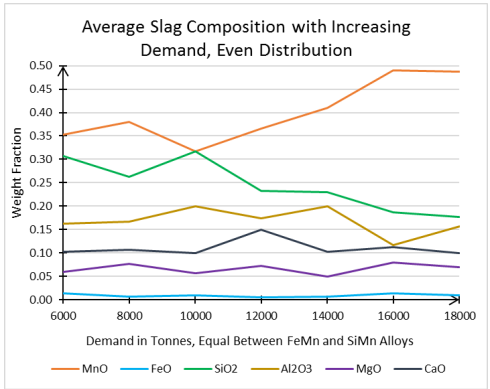

Figure 7: Average slag composition across all HC FeMn furnaces for increasing demand. Equal demand for each end-product.

The slag-to-metal ratio is 0.68 - 0.71 for demands less than 12 000 tonnes. For greater demands, the slag-to-metal ratio decreases to the lower bound of 0.50. Here, production of the least profitable alloy MC SiMn cannot satisfy demand as the slag-to-metal ratio decreases to release capacity in the FeMn furnaces to satisfy the increasing demand of FeMn alloys which are more profitable. At a demand of 12 000 tonnes, the FeMn production needs the capacity to

ACCEPTED MANUSCRIPT

satisfy the FeMn alloy demand. Thus, less capacity is available to produce slag. This trend continues for increasing demand until the lower bound of the slag-to-metal ratio is reached. As the slag-to-metal ratio decreases, it becomes more favourable to send slag with a higher content of MnO and lower content of SiO_2. Thus, as the volume of slag goes down, the amount of MnO increases to make the slag carry more of the important oxides to form pure metals in the MC SiMn furnace, as can be seen from Figure 7.

The results from Table 10 are for an instance where the slag-to-metal ratio is at its lower bound of 0.50. The authors suspect that the value of using the MAMP formulation is even greater in situations where the optimal slag-to-metal ratio is above the lower bound. The single furnace optimisation practice always minimises the slag-to-metal ratio, as it optimises the profit for single furnaces, consequently produces as much metal as possible. Solving the MAMP problem, on the other hand, enables optimising the metal-to-slag ratio relative to the overall profit. A larger volume of slag is therefore produced and allocated efficiently to the MC SiMn furnaces. The decision to maximise metal output in single furnace optimisation could of course also be changed to maximise slag output, but this is not a trivial decision to make simply by consulting raw material costs and end-product revenues.

6. Concluding Remarks

This paper has presented an optimisation model for manganese alloy multi-plant production (MAMP) planning as a nonlinear pooling problem, and outlined a global optimisation algorithm by means of a Multiparametric Disaggregation Technique (MDT). The computational study from Eramet Norway shows that the proposed solution approach can solve MAMP problem sizes of up to seven furnaces spread across three plants to within a global optimality gap of 3% for a run time of four hours. These results demonstrate that the MDT scales well with larger problem instances, thus supporting earlier computational results of the MDT as a promising method for large-scale nonconvex bilinear problems. Yet, for large problem sizes, the precision level of the discretisation is decisive for the numerical efficiency.

Solving the production planning holistically as a multi-plant problem outperforms the current operational practice of single furnace optimisation. Moreover, the incorporation of a spot market visualises which products are most profitable since these are the products produced after the fixed demand is met. By minimising power consumption and accounting for CO and CO_2 emissions, the proposed production-planning model may facilitate new manganese production strategies that ensure sustainable resources utilisation and lower emissions, thereby aligning with the increasing focus on environmental impacts caused by production from energy-intensive industries *(United Nations, 2016; Figueres et al., 2017)*. Further work on the problem and solution approach studied in the paper includes accounting for uncertainty in market demand and raw material availability, as well as including furnace configuration as a decisions variable.

ACCEPTED MANUSCRIPT

7. Acknowledgements

The authors gratefully acknowledge input and support to the model development and case studies from Benjamin Ravary and Helge Øsenstad, Eramet Norway. SOW and BRK gratefully acknowledge support from NFR grant 228460/030.

References

Alfaki, M., 2012. Models and solution methods for the pooling problem. Ph.D. thesis. The University of Bergen.

Alfaki, M., Haugland, D., 2013. Strong formulations for the pooling problem. Journal of Global Optimization 56, 897–916.

Amos, F., Rönnqvist, M., Gill, G., 1997. Modelling the pooling problem at the New Zealand Refining Company. Journal of the Operational Research Society 48, 767–778.

Audet, C., Brimberg, J., Hansen, P., Digabel, S.L., Mladenović, N., 2004. Pooling problem: Alternate formulations and solution methods. Management Science 50, 761–776.

Ben-Tal, A., Eiger, G., Gershovitz, V., 1994. Global minimization by reducing the duality gap. Mathematical Programming 63, 193–212.

Boland, N., Kalinowski, T., Rigterink, F., Savelsbergh, M., 2015. A special case of the generalized pooling problem arising in the mining industry. Optimization Online e-prints .

Castro, P.M., Teles, J.P., 2013. Comparison of global optimization algorithms for the design of water-using networks. Computers & Chemical Engineering 52, 249–261.

d'Harambure, A., 2015. Overview of the global manganese industry. URL: http://www.manganese.org/images/uploads/board-documents/14._2015_AC_-_Aloys_dHarambure.pdf. Accessed 03.09.2016.

Figueres, C., Schellnhuber, H.J., Whiteman, G., Rockstrøm, J., Hobley, A., Rahmstorf, S., 2017. Three years to safeguard our climate. Nature 546, 593–595.

Haverly, C.A., 1978. Studies of the behavior of recursion for the pooling problem. ACM Sigmap Bulletin , 19–28.

International Manganese Institute and Hatch, 2015. The environmental profile of manganese alloys. URL: http://www.manganese.org/images/uploads/pdf/IMnI_LCA_Summary_Report_View_2015.pdf. Accessed 07.09.2016.

InvestmentMine, 2017. Historical manganese prices and price chart. URL: http://www.infomine.com/investment/metal-prices/manganese/all/. Accessed 25.03.2017.

Jezowski, J., 2010. Review of water network design methods with literature annotations. Industrial & Engineering Chemistry Research 49, 4475–4516.

Jipnang, E., Monheim, P., Oterdoom, H., 2013. Process optimisation model for FeMn and SiMn production, in: The Thirteenth International Ferroalloys Congress, Efficient Technologies in Ferroalloy Industry, Almaty, Kazakhstan, pp. 811–820.

Kolodziej, S., Castro, P.M., Grossmann, I.E., 2013a. Global optimization of bilinear programs with a multiparametric disaggregation technique. Journal of Global Optimization 57, 1039–1063.

Kolodziej, S.P., Grossmann, I.E., Furman, K.C., Sawaya, N.W., 2013b. A discretization-based approach for the optimization of the multiperiod blend scheduling problem. Computers & Chemical Engineering 53, 122–142.

Meyer, C.A., Floudas, C.A., 2006. Global optimization of a combinatorially complex generalized pooling problem. AIChE journal 52, 1027–1037.

Misener, R., Floudas, C.A., 2009. Advances for the pooling problem: modeling, global optimization, and computational studies. Applied and Computational Mathematics 8, 3–22.

Olsen, S.E., Olsen, S., Tangstad, M., Lindstad, T., 2007. Production of manganese ferroalloys. Tapir Academic Press.

Quesada, I., Grossmann, I.E., 1995. Global optimization of bilinear process networks with multicomponent flows. Computers & Chemical Engineering 19, 1219–1242.

ACCEPTED MANUSCRIPT

Sherali, H.D., Adams, W.P., Driscoll, P.J., 1998. Exploiting special structures in constructing a hierarchy of relaxations for 0-1 mixed integer problems. Operations Research 46, 396–405.

Tawarmalani, M., Sahinidis, N.V., 2002. Convexification and global optimization in continuous and mixed-integer nonlinear programming: theory, algorithms, software, and applications. volume 65. Springer Science & Business Media.

Teles, J.P., Castro, P.M., Matos, H.A., 2012. Global optimization of water networks design using multiparametric disaggregation. Computers & Chemical Engineering 40, 132–147.

Teles, J.P., Castro, P.M., Matos, H.A., 2013. Multi-parametric disaggregation technique for global optimization of polynomial programming problems. Journal of Global Optimization 55, 227–251.

United Nations, 2016. Changing consumption patterns. URL: http://www.unep.org/Documents.Multilingual/Default.asp?DocumentID=52&ArticleID=52. Accessed 06.12.2016.

Wicaksono, D.S., Karimi, I.A., 2008. Piecewise MILP under- and overestimators for global optimization of bilinear programs. AIChE Journal 54, 991–1008.

A. Main furnace reactions

The main chemical reactions taking place in the furnaces during producing of HC FeMn and MC SiMn, respectively, are (Olsen et al., 2007)

$$2\,MnO_2(s) + CO(g) \longrightarrow Mn_2O_3(s) + CO_2(g) \tag{70}$$

$$3\,Mn_2O_3(s) + CO(g) \longrightarrow 2\,Mn_3O_4(s) + CO_2(g) \tag{71}$$

$$Mn_3O_4(s) + CO(g) \longrightarrow 3\,(MnO) + CO_2(g) \tag{72}$$

$$(MnO) + C(s) \longrightarrow \underline{Mn} + CO(g) \tag{73}$$

$$C(s) \longrightarrow \underline{C} \tag{74}$$

$$3\,Fe_2O_3(s) + CO(g) \longrightarrow 2\,Fe_3O_4(s) + CO_2(g) \tag{75}$$

$$Fe_3O_4(s) + CO(g) \longrightarrow 3\,(FeO) + CO_2(g) \tag{76}$$

$$(FeO) + C(s) \longrightarrow \underline{Fe} + CO(g) \tag{77}$$

$$(SiO_2) + 2\,C(s) \longrightarrow \underline{Si} + 2\,CO(g) \tag{78}$$

$$C(s) + CO_2(g) \longrightarrow 2\,CO(g) \tag{79}$$

$$Al_2O_3(s) \longrightarrow (Al_2O_3) \tag{80}$$

$$MgO(s) \longrightarrow (MgO) \tag{81}$$

$$CaO(s) \longrightarrow (CaO) \tag{82}$$

The parentheses denote the slag phase and underlines the metal phase.